Background Heterogeneity and Other Uncertainties in Estimating Urban Methane Flux: Results from the Indianapolis Flux (INFLUX) Experiment

Nikolay V. Balashov[1], Kenneth J. Davis[1], Natasha L. Miles[1], Thomas Lauvaux[1,2], Scott J. Richardson[1], Zachary R. Barkley[1], Timothy A. Bonin[3, 4]

[1]The Pennsylvania State University, University Park, Pennsylvania, USA
[2]Laboratory of Climate Sciences and Environment, Gif-sur-Yvette, France
[3]Cooperative Institute for Research in Environmental Sciences, Boulder, Colorado, USA
[4]Chemical Sciences Division, National Oceanic and Atmospheric Administration, Boulder, Colorado, USA

Abstract

As natural gas extraction and use continues to increase, the need to quantify emissions of methane (CH_4), a powerful greenhouse gas, has grown. Large discrepancies in Indianapolis CH_4 emissions have been observed when comparing inventory, aircraft mass-balance, and tower inverse modeling estimates. Four years of continuous CH_4 mole fraction observations from a network of nine towers as a part of the Indianapolis Flux Experiment (INFLUX) are utilized to investigate four possible reasons for the abovementioned inconsistencies: (1) differences in definition of the city domain, (2) a highly temporally variable and spatially non-uniform CH_4 background, (3) temporal variability in CH_4 emissions, and (4) the presence of unknown CH_4 sources. Reducing the Indianapolis urban domain size to be consistent with the inventory domain size decreases the CH_4 emission estimation of the inverse modeling methodology by about 35% and thereby lessens the discrepancy by bringing total city flux within an error range of one of the inventories. Nevertheless, the inverse modeling estimate still remains about 40% higher than the inventory value. Hourly urban background CH_4 mole fractions are shown to be heterogeneous and temporally variable. Variability in a single point background mole fractions observed at any given moment could be up to about 50 ppb depending on a wind direction, but

30 decreases substantially when averaged over multiple days. Statistically significant, long-term
31 biases in background mole fractions of 2-5 ppb are found from single point observations from
32 most wind directions. Boundary layer budget estimates suggest that Indianapolis CH_4 emissions
33 did not change significantly when comparing 2014 to 2016. However, it appears that CH_4
34 emissions may follow a diurnal cycle with daytime emissions (12-16 LST) approximately twice
35 as large as nighttime emissions (20-5 LST). No significant unknown CH_4 sources are found.
36 The data from the towers suggest that the strongest CH_4 source in Indianapolis is South Side
37 Landfill. Other sources, such as leaks from the natural gas (NG) distribution system, are
38 localized and transient, and do not appear to be a consistently large source of CH_4 emissions in
39 Indianapolis. However, some uncertainty regarding occasional significant CH_4 leaks from NG
40 distribution exists. Long-term averaging, spatially-extensive upwind mole fraction observations,
41 mesoscale atmospheric modeling of the regional emissions environment, and careful treatment of
42 the times of day and areal representation of emission estimates are recommended for precise and
43 accurate quantification of urban CH_4 emissions.
44
45 **1 Introduction**
46 From the beginning of the Industrial Revolution to 2011, atmospheric methane (CH_4) mole
47 fractions increased by a factor of 2.5 due to anthropogenic processes such as fossil fuel
48 production, waste management, and agricultural activities (Ciais et al., 2013). The increase in
49 CH_4 is a concern as it is a potent greenhouse gas (GHG) with a global warming potential 28-34
50 times greater than that of CO_2 over a period of 100 years (Myhre et al., 2013). The magnitudes
51 of component CH_4 sources, and the causes of variability in the global CH_4 budget, however, are
52 not well understood although there is some evidence that biogenic emissions may play an

53 important role in the recent CH_4 increases (Nisbet et al., 2016; Saunois et al., 2016). Improved
54 understanding of CH_4 emissions is needed (National Academies of Sciences and Medicine,
55 2018).

56 In particular, the estimates of continental U.S. anthropogenic CH_4 emissions disagree.
57 Inventories from Environment Protection Agency (EPA) and Emissions Database for Global
58 Atmospheric Research (EDGAR) in 2008 reported emission values of 19.6 and 22.1 TgC y^{-1}
59 (Miller et al., 2013). However, top-down methodologies using aircraft and inverse modeling
60 framework found emission values of 32.4 ± 4.5 TgC y^{-1} for 2004 and 33.4 ± 1.4 TgC y^{-1} for
61 2007-2008 respectively (Kort et al., 2008; Miller et al., 2013). Underestimation of natural gas
62 (NG) production and agricultural sources are possible reasons for this disagreement (Miller et al.,
63 2013; Brandt et al., 2014; Jeong et al., 2014). Efforts to reconcile GHGs emissions estimates
64 using atmospheric methods and inventory assessment have sometimes succeeded (Schuh et al.,
65 2013; Zavala-Araiza et al., 2015; Turnbull et al., 2019) when careful attention is given to the
66 details of each method, and targeted atmospheric data are available. A recent synthesis of
67 emissions from the U.S. NG supply chain demonstrated similar success and concluded that
68 current inventory estimates of emissions from U.S. NG production are too low and that emission
69 from NG distribution is one of the greatest remaining sources of uncertainty in the NG supply
70 chain (Alvarez et al., 2018).

71 Due to the uncertainties in CH_4 emissions from NG distribution it is natural that urban
72 emissions are of interest as well. For example, studies indicate that ~60-100% of Boston CH_4
73 emissions are attributable to the NG distribution system (McKain et al., 2015; Hendrick et al.,
74 2016). Recent studies of urban CH_4 emissions in California indicate that the California Air
75 Resources Board (CARB) inventory tends to underestimate the actual CH_4 urban fluxes possibly

due to fugitive emissions that result from the NG infrastructures common to the urban environments (Wunch et al., 2009; Jeong et al., 2016; Jeong et al., 2017). The accuracy and precision of atmospheric estimates of urban CH_4 emissions are limited by available atmospheric observations (Townsend-Small et al., 2012), potential source magnitude variability with time (Jackson et al., 2014; Lamb et al., 2016), errors in atmospheric transport modeling (Hendrick et al., 2016; Deng et al., 2017; Sarmiento et al., 2017), and complexity in atmospheric background conditions (Cambaliza et al., 2014; Karion et al., 2015; Heimburger et al., 2017). In this work, detailed analysis of urban CH_4 mole fractions is performed for the city of Indianapolis to better understand the aforementioned uncertainties of urban CH_4 emissions.

The Indianapolis Flux Experiment (INFLUX; Davis et al., 2017) is a testbed for improving quantification of urban GHGs emissions and their variability in space and time. INFLUX (http://influx.psu.edu) is located in Indianapolis partly because of its isolation from other urban centers and the flat Midwestern terrain. It includes a very dense GHGs monitoring network, comprised of irregular insitu aircraft measurements (Heimburger et al., 2017; Cambaliza et al., 2014), continuous in situ observations from communications towers using cavity ring-down spectroscopy (Richardson et al., 2017; Miles et al., 2017), and automated flask sampling systems for quantification of a wide variety of trace gases (Turnbull et al., 2015). Meteorological sensors include a Doppler lidar providing continuous boundary layer depth and wind profiles, and tower-based eddy covariance measurements of the fluxes of momentum, sensible and latent heat (Sarmiento et al., 2017). The network is designed for emissions estimates using top-down methods such as tower-based inverse modeling (Lauvaux et al., 2016) and aircraft mass balance estimates (Cambaliza et al., 2015).

98 Lamb et al. (2016) compared Indianapolis CH_4 emissions estimates from a variety of
99 approaches, which are inventory, aircraft mass balances, and inverse modeling. The results
100 revealed large mean differences among the city fluxes estimated from these methods (Fig. 1). In
101 general, the inventory methods arrived at lower estimates of emissions compared to the
102 atmospheric, or top-down approaches. CH_4 fluxes calculated using the aircraft mass balance
103 technique varied considerably between flights, more than would be expected from propagation of
104 errors of the component measurements (Cambaliza et al., 2014; Lamb et al., 2016). The
105 atmospheric inverse estimate was significantly higher than the inventory and some of the
106 aircraft-derived values.
107 Biogenic emissions from the city are dominated by a landfill close to downtown, and
108 these emissions are thought to be fairly well known (GHG reporting program). Although
109 evidence of possible variability in landfill emissions exists from Cambaliza et al. (2015) study
110 that used aircraft mass balance on five different occasions to calculate CH_4 flux from this
111 landfill. Uncertainty in total city emissions is mainly driven by the uncertainty in thermogenic
112 emissions, which are hypothesized to emerge largely from the NG distribution system (Mays et
113 al., 2009; Cambaliza et al., 2015; Lamb et al., 2016). This uncertainty has not yet been resolved.
114 In this study, we explore potential explanations for the discrepancies in CH_4 emissions estimates
115 from Indianapolis and posit methods and recommendations for the study of CH_4 emissions from
116 other urban centers.
117 We examine four different potential explanations for the CH_4 flux discrepancies reported
118 in Lamb et al. (2016): (1) inconsistent geographic boundaries, (2) heterogeneity in the urban-
119 scale CH_4 background, (3) temporal variability in urban emissions, and (4) CH_4 sources that are
120 not accounted for in the inventories. Well-calibrated CH_4 sensors on the INFLUX tower network

121 (Miles et al., 2017) collected continuous CH_4 observations from 2013 to 2016 and provide a
122 unique opportunity to explore these issues.
123
124 **2 Methods**
125
126 **2.1 Experimental site**
127 This study uses data from a tower-based GHG observational network located in the city and
128 surrounding suburbs of Indianapolis, Indiana in the Midwestern U.S. Prior studies have used
129 varying definitions for the region of Indianapolis (Cambaliza et al., 2015, Lamb et al., 2016). In
130 this work, we follow Gurney et al. (2012) and define Indianapolis as the area of Marion County.
131 The flat terrain of the region simplifies interpretation of the atmospheric transport. The land-
132 surface heterogeneity inherent in the urban environment (building roughness, spatial variations in
133 the surface energy balance) does have a modest influence on the flow within the city and the
134 boundary layer depth difference between the urban and rural areas (Sarmiento et al., 2017).
135 Figure 2 shows two domains that have been used for the evaluation of Indianapolis CH_4
136 emissions (Lamb et al., 2016; Lauvaux et al., 2016). The first domain is the whole area shown in
137 the figure enclosing both Indianapolis and places that lie outside of its boundaries. This domain
138 has been used for the inversion performed in Lamb et al. (2016). The second domain is Marion
139 County outlined with a green dashed line. It is assumed here that this domain is much more
140 representative of the actual Indianapolis municipal boundaries as this area encompasses the
141 majority of the urban development associated with the city of Indianapolis (Gurney et al., 2012).
142 The larger domain has three additional landfills that based on the EPA gridded inventory
143 (Maasakkers et al., 2016) increase Indianapolis CH_4 emissions by about 50% when compared to

144 the smaller domain. The inversion explained in Lamb et al. (2016) has been rerun for two of the
145 domains mentioned above and the results (Fig. 1) have been reexamined.
146
147 **2.2 INFLUX tower network**
148 The continuous GHG measurements from INFLUX are described in detail in Richardson et al.
149 (2017). The measurements were made using wavelength-scanned cavity ring down
150 spectrometers (CRDS, Picarro, Inc., models G2301, G2302, G2401, and G1301), installed at the
151 base of existing communications towers, with sampling tubes secured as high as possible on each
152 tower (39 – 136 m above ground level (AGL); Miles et al., 2017). A few towers also included
153 measurements at 10 m AGL and one or two intermediate levels. While INFLUX tower in-situ
154 measurements began in September 2010, here we focus on the CH_4 measurements from 2013 –
155 2016. From June through December 2012, there were two or three towers with operational CH_4
156 measurements. By July 2013, five towers included measurements of CH_4, and throughout the
157 majority of the years 2015 – 2016 there were eight INFLUX towers with CH_4 measurements
158 (Fig. 3). Flask to in-situ comparisons and round-robin style testing indicated compatibility
159 across the tower network of 0.6 ppb CH_4 (Richardson et al., 2017). In this study we use hourly
160 means of CH_4, which were reported on the WMO X2004A scale.
161
162 **2.3 Meteorological data**
163 Wind data was measured at the Indianapolis International Airport (KIND), Eagle Creek Airpark
164 (KEYE), and Shelbyville Municipal Airport (KGEZ). The data used are hourly values from the
165 Integrated Surface Dataset (ISD) (https://www.ncdc.noaa.gov/isd) and 5-minute values directly
166 from the Automated Surface Observing System (ASOS). A complete description of ASOS

stations is available at https://www.weather.gov/media/asos/aum-toc.pdf. The accuracy of the wind speed is ±1 m/s or 5% (whichever is greater) and the accuracy of the wind direction is 5 degrees when the wind speed is ≥ 2.6 m/s. The anemometers are located at about 10 meters AGL. The wind data reported in ISD are given for a single point in time recorded within the last 10 minutes of an hour and are closest to the value at the top of the hour.

The planetary boundary layer height (BLH) was determined from a Doppler lidar deployed in Lawrence, Indiana about 15 km to the northeast of downtown. The lidar is a Halo Streamline unit, which was upgraded to have extended range capabilities in January 2016. The lidar continuously performs a sequence of conical, vertical-slice, and staring scans to measure profiles of the mean wind, turbulence, and relative aerosol backscatter. All of these measurements are combined using a fuzzy-logic technique to automatically determine the BLH continuously every 20-min (Bonin et al., 2018). The BLH is primarily determined from the turbulence measurements, but the wind and aerosol profiles are also used to refine the BLH estimate. The BLHs are assigned quality-control flags that can be used to identify times when the BLH is unreliable, such as when the air is exceptionally clean, the BLH is below a minimum detectable height, or clouds and fog that attenuate the lidar signal exist. Additional details about the algorithm and the lidar operation for the INFLUX project are provided in Bonin et al. (2018). Doppler lidar measurements are available at https://www.esrl.noaa.gov/csd/projects/influx/.

2.4 Urban methane background

Both aircraft mass balance and inverse modeling methodologies rely on an accurate estimation of the urban CH_4 enhancement relative to the urban CH_4 background in order to produce a reliable

189 flux estimate (Cambaliza et al., 2014; Lamb et al., 2016). The CH_4 mole fraction enhancement is
190 defined as,

$$C_{enhancement} = C_{downwind} - C_{bg} \quad (1)$$

191 where $C_{downwind}$ is the CH_4 mole fraction measured downwind of a source and C_{bg} is the CH_4
192 background mole fraction, which can be measured upwind of the source, but this is not
193 necessary. Background, as defined in this body of literature, is a mole fraction measurement that
194 does not contain the influence of the source of interest, but which is assumed to accurately
195 represent mole fractions that are upwind of the source of interest and measured simultaneously
196 with the downwind mole fractions.

197 Aircraft mass balance studies at Indianapolis mentioned in this article used two main
198 methods to determine a background value. The first method calculates an average of the aircraft
199 transect edges that lie outside of the city domain (Cambaliza et al., 2014). In the second
200 approach, a horizontally varying background is introduced by linearly interpolating median
201 background values of each of the transect edges (Heimburger et al., 2017). In theory there is also
202 a third method that uses an upwind transect as a background field, but in the studies above it was
203 assumed that the edges are representative of an upwind flow. In the case of an inversion, it is
204 common to pick a tower that is located generally away from urban sources and has on average
205 the smallest overall enhancement (Lavaux et al., 2016). Because choosing the background
206 involves a degree of subjectivity (Heimburger et al., 2017) we consider how these choices may
207 influence emission estimates and introduce error, both random and systematic, using data from
208 the INFLUX tower network.

209 Using tower network data from November 2014 through the end of 2016, two CH_4
210 background fields are generated for the city of Indianapolis based on two different sets of

criteria. The notion is based on the fact that a choice of background is currently rather arbitrary in the literature (Heimburger et al., 2017) and at every point in time it is possible to choose multiple background values that are equally acceptable for the flux estimation. In our case both approaches identify a tower suitable to serve as a background for each of the eight wind directions (N, NE, E, SE, S, SW, W, NW), where an arc of 45° represents a direction (e.g. winds from N are between 337.5° and 22.5°). Estimating background for different wind directions is implemented to more accurately represent upwind flow that is hopefully not contaminated by local sources.

Criterion 1 corresponds to a typical choice of a background in a case of tower inversion and is based on the concept that the lowest CH_4 mole fraction measured at any given time is not affected by the city sources and therefore is a viable approximation of the background CH_4 mole fractions outside of the city (Miles et al., 2017; Lauvaux et al., 2016). Given this assumption, the tower with the lowest median of the CH_4 enhancement distribution (calculated by assuming the lowest measurement among all towers at a given hour as a background) for each of the wind directions over the November 2014 through December 2016 time period is chosen as a background site (Miles et al., 2017). Criterion 2 requires that the tower is outside of Marion County (outside of the city boundaries) and is not downwind of any known regional CH_4 source (Fig. 2). For some wind directions, there are multiple towers that could qualify as a background; we pick towers in such a manner that they are different for each criterion given a wind direction in order to calculate the error associated with the use of different but acceptable backgrounds. The towers used for both criteria and for each of the eight wind directions are displayed in Table 1. Quantifying differences between these two backgrounds allows for an opportunity to better

understand the degree of uncertainty that exists in the atmospheric CH_4 background at Indianapolis.

To make the comparison as uniform as possible only data from 12-16 LST are utilized (all hours are inclusive) when the boundary layer is typically well-mixed (Bakwin et al., 1998). A lag 1 autocorrelation is found between 12-16 LST hours, i.e. the hourly afternoon data are correlated to the next hour, but the correlation is not significant for samples separated by two hours or more. Therefore, hours 13 and 15 LST are eliminated to satisfy the independence assumption for hourly samples. Furthermore, we make an assumption that the data satisfy steady state conditions. If the difference between consecutive hourly wind directions exceeds 30 degrees or the difference between hours 16 and 12 LST exceeds 40 degrees, the day is eliminated. Days with average wind speeds below 2 m/s are also eliminated due to slow transport (the transit time from tower 1 to tower 8 is about 7 hours at a wind speed of 2 m/s).

2.5 Frequency and bivariate polar plots

Frequency and bivariate polar plots are used in this work to gain more knowledge regarding CH_4 background variability based on criteria 1 and 2, and to identify sources located within the city. To generate these polar plots, we use the *openair* package (from R programming language) created specifically for air quality data analysis (Carslaw and Ropkins, 2012). Bivariate and frequency polar plots indicate the variability of a pollutant concentration at a receptor (such as an observational tower) as a function of wind speed and wind direction, preferably measured at the location of the receptor or within several kilometers of the receptor. The frequency polar plot is generated by partitioning the CH_4 hourly data into the wind speed and direction bins of 1 m s^{-1} and 10° respectively. To generate bivariate polar plots, wind components u and v are calculated

for hourly CH_4 mole fraction values, which are fitted to a surface using a Generalized Additive Model (GAM) framework in the following way,

$$\sqrt{C} = \beta + s(u, v) + \epsilon \quad (2)$$

where C is the CH_4 mole fraction transformed by a square root to improve model diagnostics such as a distribution of residuals, β is mean of the response, s is the isotropic smoothing function of the wind components u and v, and ϵ is the residual. For more details on the model see Carslaw and Beevers (2013).

2.6 Temporal variability and approximate flux estimation

Temporal variability may play an important role in the quantification of urban CH_4 emissions. Lamb et al., (2016) suggested that temporal variability might partially explain the differences among CH_4 flux estimates shown in Figure 1. If temporal variability of CH_4 emissions exists within the city, disagreements in the CH_4 flux between studies could be attributed to differences in their sampling period. Because the INFLUX tower data at Indianapolis contain measurements at all hours of the day over multiple years, we can utilize this dataset to better understand the temporal variability in methane emissions in the city.

We apply a simplified atmospheric boundary layer budget, not to estimate precisely the actual city emissions, but rather to evaluate temporal variability of the emissions. We begin by assuming CH_4 emissions Q_a (mass per unit time per unit area) are not chemically active and are constant over a distance Δx spanning a significant portion of the city. The next assumption is that a CH_4 plume measured upwind of the city is well mixed within a layer of depth H (which is the same as BLH). We treat wind speed u as constant within the layer for every hour considered.

Given the above-mentioned assumptions we can write a continuity equation describing mass conservation of CH_4 concentration C within a box in the following fashion,

$$\Delta x H \frac{\partial C}{\partial t} = \Delta x Q_a + uH(C_b - C) + \Delta x \frac{\partial H}{\partial t}(C_a - C) \quad (3)$$

where C_b is the CH_4 concentration upwind of the city (or background), and C_a is the CH_4 concentration above the mixed layer (Hanna et al., 1982; Arya, 1999; Hiller et al., 2014). The left hand of the equation represents the change in CH_4 concentration with time, $\Delta x Q_a$ denotes a constant CH_4 source over the distance Δx, $uH(C_b - C)$ indicates a change of CH_4 concentration due to horizontal advection, and finally $\Delta x \frac{\partial H}{\partial t}(C_a - C)$ term accounts for the vertical advection and encroachment processes that result from changing BLH. By assuming steady state conditions ($\frac{\partial C}{\partial t} = 0$ and $\frac{\partial H}{\partial t} = 0$), the equation can be simplified to

$$Q_a = \frac{uH(C - C_b)}{\Delta x} \quad (4)$$

We use equation 4 to estimate hourly CH_4 emissions (Q_a) from Indianapolis (see assumptions in the paragraph below) given hourly averaged data of H from the lidar positioned in the city, wind speed (u) from the local weather stations, and upwind (C_b) and downwind (C) CH_4 mole fractions measured (and then converted to concentrations) at towers 1, 8, and 13 (depending on a wind direction) using data from heights of 40 m, 41 m, and 87 m respectively (see Fig. 2).

The CH_4 concentrations are derived from CH_4 mole fractions by approximating average molar density of dry air (in mol m^{-3}) within the boundary layer for every hour of the day, where variability of pressure with altitude is calculated using barometric formula and it is assumed that temperature decreases with altitude by 6.5 K per kilometer. The hourly surface data for pressure and temperature is taken from KIND weather station. The difference between concentrations

297 $C - C_b$ is instantaneous and not lagged, where C_b represents air parcel entering the city and C
298 represents the same air parcel exiting the city (Turnbull et al., 2015). The CH_4 enhancements
299 $C - C_b$ are estimated for daytime by averaging observations spanning 12-16 LST and for
300 nighttime by averaging observations spanning 20-5 LST. These time periods are based on lidar
301 estimations of when on average H varies the least. The day and night were required to contain at
302 least 3 and 9 hourly CH_4 values respectively for averaging to occur, otherwise the day/night is
303 eliminated. Observations when H is below 100 m are not used to avoid the cases when
304 measurements from towers may be above the boundary layer. In order to better achieve the
305 assumption that the boundary layer is fully mixed (especially at night), all hours with wind
306 speeds below 4 m/s are eliminated (Van De Wiel., 2012). To approximate the emissions of the
307 whole city we need to know the approximate area of the city and the distance over which the
308 plume is affected by the city CH_4 sources. The area of the city is about 1024 km^2 (the area of
309 Marion County) and the length that plume traverses when it is over the city ranges from 32 to 35
310 km depending on which downwind tower is used. We assume that CH_4 measurements at towers
311 8 and 13 are representative of a vertically well-mixed city plume as the towers are located
312 outside of the city boundaries and allow for sufficient vertical mixing to occur. For S and SW
313 wind directions tower 8 observations are used to represent downwind conditions with
314 background observations coming from towers 1 and 13, respectively (based on criterion 1 shown
315 in Table 1). For W wind direction, tower 13 observations represent the downwind with
316 background obtained from tower 1. The wind direction is required to be sustained for at least 2
317 hours, otherwise the data point is eliminated.
318
319 **2.7 Indianapolis CH_4 sources**

Only a few known CH_4 point sources exist within Indianapolis (Cambaliza et al., 2015, Lamb et al., 2016). The Southside Landfill (SSLF), located near the center of the city, is thought to be the largest point source in the city with emissions ranging between about 28 mol/s (inventory from Maasakkers et al., 2016 and GHG reporting program) and 45 mol/s (aircraft; Cambaliza et al., 2015) depending on an emission estimation methodology. SSLF could account for as little as 33% (top-down from Cambaliza et al., 2015) or as much as 63% (invetnory from Maasakkers et al., 2016) of total Marion County CH_4 emissions contigent on how much of the total city emissions are coming from NG. Other city point sources are comparatively small; the wastewater treatment facility located near SSLF contributes about 3-7 mol/s (inventory from Lamb et al. 2016), and the transmission-distribution transfer station at Panhandle Eastern Pipeline (also known as a city gate and further in this study abbreviated as PEP) is estimated to be about 1 mol/s (inventory from Lamb et al. 2016). The remaining CH_4 sources, mainly from NG and livestock, are considered to be diffuse sources and are not well known. Potential sources of emissions related to NG activities include gas regulation meters, emissions from transmission and storage, and Compressed Natural Gas (CNG) fleets. These diffuse NG sources account for 21-67% (this value varies due to the uncertainty in SSLF emissions) of the city emissions or 20 mol/s (inventory from Maasakkers et al., 2016) to 64 mol/s (top down from Cambaliza et al., 2015). Livestock emissions for Marion County are estimated to be around 1.5 mol/s (inventory from Maasakkers et al., 2016). An important question remains of whether SSLF or NG is the dominant CH_4 source in Indianapolis. There could also be a possibility of temporal variability in either of the sources as described in the section above.

3 Results and discussion

3.1 Inversion and city boundaries

345 A significant portion of CH_4 emissions across the U.S. can be characterized by numerous large
346 point sources scattered throughout the country rather than by broad areas of smaller
347 enhancements (Maasakkers et al., 2016). Because of this, the total emissions for a given domain
348 can be very sensitive to how that domain is defined. A small increase or decrease in the domain
349 area could add or remove a large point source and significantly impact the total emissions
350 defined within the domain.

351 In the case of Indianapolis, this issue became apparent when the emissions were
352 calculated using an atmospheric inversion model (Lamb et al., 2016; Lauvaux et al., 2016). The
353 atmospheric inversion solved for fluxes in domain 1 (Fig. 2), which significantly increased the
354 estimated emissions in comparison with the inventory values that were gathered mainly within
355 Marion County (domain 2). When reduced to domain 2, inverse modeling emission estimates
356 decrease to 107 mol/s, which falls within an error bar of Lamb et al. (2016) inventory estimate.
357 This difference is significant and could at least partially explain the discrepancy shown in Figure
358 1 between the emission values from the inventories and emission results from the inverse
359 modeling. However, even the decreased inverse modeling estimate is about 40% higher than the
360 inventories.

361 It is difficult for us to critically assess this result without performing complex sensitivity
362 analysis with this inversion system (which is not the goal of this article), but it is important to
363 note that inverse modeling is prone to errors in prior, background, and meteorological transport.
364 Also, Figure 3 indicates that tower data were sparse in 2012-2013 perhaps contributing to
365 potential error in the inversion.

366 Additionally, the subject of the domain is relevant for airborne mass balance flights
367 because a priori the magnitude and variability of background plume is unknown and could be

368 easily influenced by upwind sources. The issue of background is discussed further in the next
369 section.
370
371 **3.2 Variability in CH_4 background**
372 Comparisons between criterion 1 and criterion 2 CH_4 background mole fractions as a
373 function of wind speed and direction are visualized using frequency and bivariate polar plots
374 (Fig. 4). Both backgrounds generally agree on the higher CH_4 originating from the SW, SE, and
375 E wind directions (Figs. 4c-f); however, the values themselves differ especially when winds are
376 from NW, SW, and SE. As background difference plots (Figs. 4g-h) indicate, there is a
377 noticeable variability between the magnitudes of the CH_4 backgrounds, where criterion 2, by
378 design, typically has higher background mole fractions. The background differences, at a given
379 hour, suggest that the CH_4 field enveloping the city is heterogeneous with differences between
380 towers ranging from 0 to over 45 ppb (Fig. 4g). Because large gradients in CH_4 background over
381 the city could pose challenges for flux estimations using top down methods such as inverse
382 modeling and aircraft mass balance, it is imperative to establish whether the background
383 differences vary randomly or systematically and how to choose a background to minimize these
384 errors.
385 To further understand the nature of background variability we calculate the mean,
386 standard deviation, and standard error of background hourly differences between criterion 2 and
387 criterion 1 from November 2014 to December 2016 for each of the eight wind directions
388 mentioned in Table 1. The results are shown in Figure 5. Systematic bias is evident for the SE,
389 S, SW, W, and NW wind sectors, whereas random error dominates N, NE, and E wind
390 directions. Wind directions showing statistically significant bias have mean biases ranging from

391 2 to 5 ppb, with values as large as 8 ppb falling within the range of 2 × standard error. Standard
392 deviation plot indicates potential background discrepancy that can occur on any given day, where
393 W wind direction is the least variable with 2 × standard deviation close to 20 ppb, while SE wind
394 direction is the most variable with 2 × standard deviation falling at about 50 ppb.

395 Random errors in the mole fractions of background differences (biases) are also
396 important and are a function of the length of the data record. We quantify the random error in
397 the CH_4 background mole fraction differences using the bootstrap method by randomly sampling
398 2 to 150 hours (small and large sample size) of the background CH_4 differences for each of the
399 wind directions with replacement (we make the assumption that our differences are independent
400 since we eliminated lag 1 autocorrelation from the data). This sub-sampling experiment is
401 repeated 5000 times (Efron and Tibshirani, 1986). The standard deviations of the mean
402 (standard error) of the 5000 simulated differences are calculated for each wind direction. The
403 resulting standard errors of the city CH_4 background differences, multiplied by 2 to represent the
404 95% confidence intervals, are shown as a function of the length of the data record in Figure 6.
405 Because random error falls as sample size grows it makes sense to assign a threshold indicating a
406 minimum number of samples needed to achieve a theoretical precision for each wind direction.

407 One way to assign a required precision would be to make sure that the standard error
408 (random error) reaches a point where it is less than Indianapolis enhancement of about 12 ppb (a
409 higher estimate of the Indianapolis enhancement from section 3.3) by a factor of 2 when
410 combined with a bias (Table 2). Meaning that the sum of bias and standard error must be at most
411 6 ppb. In this approach each wind direction would have a different threshold because of the
412 differences in biases. For instance, given this requirement NW direction would need a random
413 error of 1 since its bias is 5. For NW direction, this threshold would require more than 150

414 samples. For N direction on the other hand, where the bias is 1, the requirement is fulfilled when
415 random error crosses 5 ppb at 74 samples. Now we consider these random and systematic errors
416 in CH_4 background differences in the context of Indianapolis urban CH_4 emissions.

417 For Indianapolis, using INFLUX tower network, we estimated that depending on sample
418 size (number of hours sampled) and wind direction, background gradient across the city over 12-
419 16 LST could vary from 0 to about 50 ppb (Fig. 5b). Given that the average afternoon CH_4
420 enhancement of the city is around 8-12 ppb (section 3.3; Fig. 7; Cambaliza et al., 2015; Miles et
421 al., 2017), the error on the estimated emissions could easily be over 100% if the analysis does not
422 approach the issue of background with enough sampling. A sample size of about 50 independent
423 hours significantly decreases background uncertainty for N, NE, E, S, and W wind directions and
424 allows for a more accurate assessment of the CH_4 emissions at Indianapolis. For CH_4 sources
425 with a significantly larger signal than their regional background, the mentioned background
426 variability becomes less impactful on results, but because Indianapolis is a relatively small
427 emitter of CH_4, and because there are relatively large sources outside of the city, uncertainties
428 due to background estimation are comparatively large. Our uncertainty assessment suggests that
429 the highly variable CH_4 emission values of Indianapolis from aircraft mass balance calculations
430 shown in Figure 1 are at least partially due to the variability in the urban CH_4 background of
431 Indianapolis.

432

433 **3.3. Temporal variability of methane enhancements and fluxes in Indianapolis**

434 Figure 7 presents average CH_4 mole fraction enhancements and flux calculations
435 (equation 4) at towers 8 and 13 for years 2014, 2016, and 2013-2016 (for the detailed
436 methodology see section 2.6). The years of 2014 and 2016 are chosen for temporal comparison

437 because they do not contain major BLH data gaps. The error bars in the figure show the standard
438 error multiplied by 2 indicating 95% confidence interval of each average.

439 One of the more interesting features in the Figure 7 is a day/night variability of CH_4
440 emissions at Indianapolis. The most prominent example of this feature is found in Figure 7c,
441 where the estimates for both years suggest that daytime emissions are approximately twice as
442 large as the emissions at night. The decrease of the CH_4 emissions at night also appears in tower
443 13, but the errors are too high in those estimates to make any definitive conclusions. A similar
444 urban CH_4 emissions diurnal variability is reported by Helfter et al. (2016) in their study of
445 GHGs for London, UK, where they attribute diurnal variation of CH_4 emissions to the NG
446 distribution network activities, fugitive emissions from NG appliances, and to temperature-
447 sensitive CH_4 emission sources of biogenic origin (such as a landfill). Taylor et al. (2018)
448 suggest that CH_4 emissions from landfills exhibit a diurnal cycle with higher emissions in early
449 afternoon and 30-40% lower emissions at night.

450 With regard to yearly temporal variability we are only able to compare years 2014 and
451 2016 due to limited BLH data for other years. Results from both towers suggest that
452 Indianapolis overall CH_4 emissions did not change significantly between 2014 and 2016.
453 Although it is important to be cautious about interpreting actual flux estimations given the
454 assumptions mentioned in section 2.6, it is interesting to note that the flux values from both
455 towers average at about 70 mol/s, which puts our value right in between inventory and inversion
456 estimates shown in Figure 1. If we assume that SSLF emissions are generally known (GHG
457 reporting program) that would indicate that emissions from NG distribution are likely to be
458 somewhat higher than both of the inventories currently estimate and consistent with higher error
459 bar of Lamb et al. (2016) calculation. Another possible scenario is that SSLF emissions are

460 higher than what is currently assumed. Given these complexities, uncertainty regarding the exact
461 emissions from NG distribution at Indianapolis still remains.
462
463 **3.4 Methane Sources in Indianapolis**
464 Bottom-up emission inventories have difficulty tracking changes in sources over time. Our
465 continuous tower network observations can monitor temporal and spatial variability in sources of
466 CH_4 in Indianapolis. To do so we employ the aforementioned bivariate polar plots to verify
467 known sources and potentially identify unknown sources across the city. We compare two time
468 periods, 2014-2015 (two full years) and 2016. Figure 8 displays bivariate polar plots of CH_4
469 enhancements using criterion 1 background at 9 INFLUX towers in Indianapolis over the two
470 years of 2014 and 2015. Figure 9 shows the same plot, but for the year 2016. Here we have
471 separated 2016 from 2014-2015 because of different results noted during this time.
472 The images reveal that the most consistent and strongest source in the city is the SSLF.
473 This is most evident from the 40+ ppb CH_4 enhancements detected at towers 7, 10 and 11
474 coming from the location of the SSLF (by triangulation). Enhancements from the landfill appear
475 to also be detectable at towers 2, 4, 5, and 13. Based on these observations it can be concluded
476 that there is no other source in Marion County comparable in strength to the SSLF. A small
477 fraction of the SSLF plume is likely due to the co-located wastewater facility, but the inventory
478 estimates suggest that the wastewater treatment facility is responsible for no more than 7% of
479 this plume (Cambaliza et al., 2015; Massakkers et al., 2016). The PEP, located in the
480 northwestern section of the city, may be partially responsible for a plume of 5-10 ppb at towers 5
481 and 11. However, the plume is less detectable using the criterion 2 background value that has
482 higher background (using tower 8 as a background) from NW wind direction (not shown),

adding uncertainty to the true magnitude of the enhancement from this source. The same is true for towers 2 and 13, which have pronounced plumes when winds are from the NW with the criterion 1 background, but when background 2 is used these plumes vanish (not shown). Such inconsistency makes it difficult to attribute these plumes to an urban source.

Another important point is the cluster of large enhancements surrounding tower 10 in 2014 - 2015. Because no other tower sees these enhancements (at least at comparable magnitudes), we believe that these plumes are the result of local NG leaks likely from residential sector of Indianapolis. These plumes are not consistent temporally or spatially as they mostly disappear in 2016, potentially indicating that they are transient and localized NG distribution leaks. It is difficult to ascertain the exact combined magnitude of these leaks since they mix together with SSLF into an aggregated city plume when observed from downwind towers such as 8 and 13. Yet, none of these leaks appear to be even remotely close in magnitude to the emissions that originate from SSLF. Thus, the diffuse NG source suspected to be twice as large as the SSLF source (Lamb et al., 2016) does not appear to be supported by these data. This assertion questions conclusions made by Cambaliza et al., (2015), who attributed most of the CH_4 emitted by Indianapolis to NG related activities. We hypothesize that the relatively high Indianapolis CH_4 emissions (see Fig. 1) reported by Cambaliza et al. (2015) are the result of the low sample size of airborne flux estimates making it prone to large random errors (see section 3.2). However, it is imperative to be careful and acknowledge the limitations of the current analysis. Our flux estimations at towers 8 and 13 discussed in the previous section do imply that emissions from NG distribution may be higher than estimated by the inventories indicating that an overall NG contribution may be comparable in strength to SSLF. This discrepancy requires further investigation.

4 Conclusions

We have examined four specific contributions to discrepancies between urban top-down and bottom-up CH_4 emission estimates from Indianapolis: domain definition, heterogeneous background mole fractions, temporal variability in emissions, and source knowledge. Results indicate that the urban domain definition is crucial for the comparison of the emission estimates among various methods. Atmospheric inverse flux estimates for Marion County, which is similar to the domain that is analyzed by inventory and airborne mass balance methodologies (Mays et al., 2009, Cambaliza et al., 2014, Lamb et al., 2016), is 107 mol/s compared to 160 mol/s that is estimated for the larger domain (Hestia inventory domain; Gurney et al., 2012). This partially explains higher emissions in inverse modeling estimates shown by Lamb et al. (2016); however, 107 mol/s is still about 40-50% higher than what EPA and Lamb et al. (2016) find in their inventories (Fig. 1). Although it is difficult to generalize with certainty regarding this particular inversion, significant errors are possible in an inversion system due to lack of data, false assumptions regarding prior, biased background, and erroneous modeled meteorological transport.

To better understand background variability at Indianapolis two different but acceptable background towers are selected based on specific criteria for each wind direction and their differences are used to assess heterogeneity of CH_4 background at Indianapolis. Background criterion 1 looks for a tower that is consistently lower than other towers, while background criterion 2 picks a tower that is outside of Marion County domain and is not downwind of any nearby sources as determined by EPA 2012 inventory. We focus on midday atmospheric conditions to avoid the complexities of vertical stratification in the stable boundary layer. The

529 midday Indianapolis atmospheric CH_4 mole fraction background is shown to be heterogeneous
530 with 2-5 ppb statistically significant biases for NW, W, SW, S and SE wind directions. Random
531 errors of background differences are a function of sample size and decrease as a number of
532 independent samples increase. Low sample volumes, such as a few hours of data from a single
533 point, are prone to random errors on the order of 10-30 ppb in the CH_4 background, similar to the
534 magnitude of the total enhancement from the city of Indianapolis, which is estimated to be on
535 average around 10-12 ppb. Longer-term sampling and/or more extensive background sampling
536 are necessary to reduce the random errors. Sample size required to reduce random errors of
537 background differences to an acceptable value for flux calculation is largely dependent on a wind
538 direction. Both bias (long-term average of background differences) and its random error are
539 important when estimating total background uncertainty. The results indicate that N, NE, E, S,
540 and W wind directions are more favorable for flux estimation and would require multiple days of
541 measurements (e.g. about 50 independent hours of measurements) to reduce background
542 uncertainty to about 6 ppb, noticeably smaller than the typical CH_4 enhancement from
543 Indianapolis. The remaining wind directions would require over 150 independent hourly
544 measurements to achieve similar precision. We also estimate that depending on a wind direction
545 for any given hour the spatial variability in background can be anywhere from 0 to 50 ppb. This
546 uncertainty in the CH_4 background may partially explain Heimburger et al. (2017) finding of
547 large variability in airborne estimates of Indianapolis CH_4 emissions. Given many samples, the
548 airborne studies converge to an average value of CH_4 flux that is noticeably closer to the
549 inventory estimates for Indianapolis than their individual components as presented in Figure 1.
550 Measurement and analysis strategies can minimize the impacts of these sources of error.
551 Spatially extensive measurement of upwind CH_4 mole fractions are recommended. For towers or

552 other point-based measurements, multiple upwind measurement locations are clearly beneficial.
553 For the aircraft mass balance approach, we recommend an upwind transect to be measured,
554 lagged in time if possible, to provide a more complete understanding of the urban background
555 conditions. Complex background conditions might suggest that data from certain days or wind
556 directions should not be used for flux calculation. Finally, a mesoscale atmospheric modeling
557 system informed with the locations of important upwind CH_4 sources can serve as a powerful
558 complement to the atmospheric data (Barkley et al., 2017). Such simulations can guide sampling
559 strategies, and aid in interpretation of data collected with moderately complex background
560 conditions.

561 With regard to temporal variability, no statistically detectable changes in the emission
562 rates were observed when comparing 2014 and 2016 CH_4 emissions. However, a large
563 difference between day and night CH_4 emissions was implied from a simple budget estimate.
564 Night (20-5 LST) emissions may be 2 times lower than the emissions during the afternoon (12-
565 16 LST) hours. Because prior estimates of top-down citywide emissions are derived using
566 afternoon-only measurements, overall emissions of Indianapolis may be lower than these studies
567 suggest. This bias may be present in studies performed in other cities as well. Our study
568 suggests that day/night differences in CH_4 emissions must be understood if regional emission
569 estimates are to be calculated correctly. Long-term, tower-based observations are an effective
570 tool for understanding and quantifying multi-year variability in urban emissions.

571 One final point addressed in this study is the location of major CH_4 sources in
572 Indianapolis. Analysis of the INFLUX observation data suggests that inventories for
573 Indianapolis are mostly accurate and that there is no clear evidence of a large, diffuse NG source
574 of CH_4 as implied by Lamb et al. (2016). The only major source in the city is SSLF and it is

observed at multiple towers. There is an evidence for occasional NG leaks, but they appear localized and limited in their strength. However, we cannot completely rule out occasional significant leaks of CH_4 from NG at Indianapolis due to the nature of our assumptions.

Overall, assessment of the CH_4 emissions at Indianapolis highlights a number of uncertainties that need to be considered in any serious evaluation of urban CH_4 emissions. These uncertainties amplify for Indianapolis since its CH_4 emissions are comparable in magnitude to the regional background flow and as our results show it may be difficult at times to distinguish noise in the background from the actual city emissions signal. The evaluation of larger CH_4 sources may be easier with respect to separating signal from background. However, all of the points raised in this work will be nonetheless relevant and need to be addressed for our understanding of urban CH_4 emissions to significantly improve.

Author Contribution

Nikolay Balashov, Kenneth Davis, and Natasha Miles developed the study and worked together on generating the main hypothesis of this work. They also wrote most of the manuscript. Nikolay Balashov wrote all of the codes and performed the analyses presented in this work as well as generated all of the figures. Natasha Miles and Scott Richardson helped with maintenance and gathering of the INFLUX tower data. They also wrote section 2.2 of the paper. Thomas Lauvaux helped with the analysis presented in Fig. 1 and section 3.1 concerning interpretation of the inversion modeling results from Lamb et al. (2016). Thomas Lauvaux also helped with repeating the inversion experiment for two different Indianapolis domains (Fig. 1). Zachary Barkley significantly contributed to discussions regarding the hypothesis and careful presentation of sections 2.6 and 3.3. Timothy Bonin provided all of the lidar data and wrote the

second part of section 2.3 regarding the lidar and the methodology used to determine planetary boundary layer heights. He also contributed to sections 2.6 and 3.3.

Competing Interests

The authors declare that they have no conflict of interest.

Acknowledgements

This research has been supported by the National Institute of Standards and Technology (project number 70NANB10H245). We would like to thank Dr. Bram Maasakkers for the helpful discussion regarding the EPA 2012 inventory and the relevant error structure. We also thank Dr. Paul Shepson and Dr. Brian Lamb for their useful input regarding airborne mass balance flights and the process of compiling an emissions inventory. Most importantly, we would like to acknowledge significant contributions of both reviewers who rigorously examined our science and noticeably improved clarity of our article.

References

Alvarez, R. A., Zavala-Araiza, D., Lyon, D. R., Allen, D. T., Barkley, Z. R., Brandt, A. R., Davis, K. J., Herndon, S. C., Jacob, D. J., Karion, A., Kort, E. A., Lamb, B. K., Lauvaux, T., Maasakkers, J. D., Marchese, A. J., Omara, M., Pacala, S. W., Peischl, J., Robinson, A. L., Shepson, P. B., Sweeney, C., Townsend-Small, A., Wofsy, S. C., and Hamburg, S. P.: Assessment of methane emissions from the U.S. oil and gas supply chain, Science, 10.1126/science.aar7204, 2018.

Arya, S. P.: Air pollution meteorology and dispersion, Oxford University Press New York, 1999.

Barkley, Z. R., Lauvaux, T., Davis, K. J., Deng, A., Miles, N. L., Richardson, S. J., Cao, Y., Sweeney, C., Karion, A., Smith, M., Kort, E. A., Schwietzke, S., Murphy, T., Cervone, G., Martins, D., and Maasakkers, J. D.: Quantifying methane emissions from natural gas

626 production in north-eastern Pennsylvania, Atmos. Chem. Phys., 17, 13941-13966,
627 10.5194/acp-17-13941-2017, 2017.
628 Bakwin, P. S., Tans, P. P., Hurst, D. F., and Zhao, C.: Measurements of carbon dioxide on very
629 tall towers: results of the NOAA/CMDL program, Tellus, 50B, 401–415, 1998.
630 Bonin, T. A., Carroll, B. J., Hardesty, R. M., Brewer, W. A., Hajny, K., Salmon, O. E., and
631 Shepson, P. B.: Doppler lidar observations of the mixing height in Indianapolis using an
632 automated composite fuzzy logic approach, Journal of Atmospheric and Oceanic
633 Technology, 35, 473-490, 10.1175/jtech-d-17-0159.1, 2018.
634 Brandt, A. R., Heath, G. A., Kort, E. A., O'Sullivan, F., Pétron, G., Jordaan, S. M., Tans, P.,
635 Wilcox, J., Gopstein, A. M., Arent, D., Wofsy, S., Brown, N. J., Bradley, R., Stucky, G.
636 D., Eardley, D., and Harriss, R.: Methane leaks from North American natural gas
637 systems, Science, 343, 733-735, 10.1126/science.1247045, 2014.
638 Cambaliza, M., Shepson, P., Bogner, J., Caulton, D., Stirm, B., Sweeney, C., Montzka, S.,
639 Gurney, K., Spokas, K., and Salmon, O.: Quantification and source apportionment of the
640 methane emission flux from the city of Indianapolis, Elem. Sci. Anth., 3, 2015.
641 Cambaliza, M. O. L., Shepson, P. B., Caulton, D. R., Stirm, B., Samarov, D., Gurney, K. R.,
642 Turnbull, J., Davis, K. J., Possolo, A., Karion, A., Sweeney, C., Moser, B., Hendricks, A.,
643 Lauvaux, T., Mays, K., Whetstone, J., Huang, J., Razlivanov, I., Miles, N. L., and
644 Richardson, S. J.: Assessment of uncertainties of an aircraft-based mass balance approach
645 for quantifying urban greenhouse gas emissions, Atmos. Chem. Phys., 14, 9029-9050,
646 10.5194/acp-14-9029-2014, 2014.
647 Carslaw, D. C., and Ropkins, K.: openair — An R package for air quality data analysis,
648 Environmental Modelling & Software, 27-28, 52-61,
649 https://doi.org/10.1016/j.envsoft.2011.09.008, 2012.
650 Carslaw, D. C., and Beevers, S. D.: Characterising and understanding emission sources using
651 bivariate polar plots and k-means clustering, Environmental Modelling & Software, 40,
652 325-329, https://doi.org/10.1016/j.envsoft.2012.09.005, 2013.
653 Ciais, P., Sabine, C., Bala, G., Bopp, L., Brovkin, V., Canadell, J., Chhabra, A., DeFries, R.,
654 Galloway, J., and Heimann, M.: Carbon and other biogeochemical cycles, in: Working
655 Group I Contribution To The IPCC Fifth Assessment Report. Climate Change 2013 - The
656 Physical Science Basis, edited by: Stocker, T. F., Qin, D., Plattner, G., Tignor, M., Allen,

S., Boschung, J., Nauels, A., Xia, Y., Bex, V., and Midgley, P., Cambridge Univ. Press, 465-570, 2013.

Davis, K. J., Deng, A., Lauvaux, T., Miles, N. L., Richardson, S. J., Sarmiento, D. P., Gurney, K. R., Hardesty, R. M., Bonin, T. A., and Brewer, W. A.: The Indianapolis Flux Experiment (INFLUX): A test-bed for developing urban greenhouse gas emission measurements, Elem. Sci. Anth., 5, 2017.

Deng, A., Lauvaux, T., Davis, K. J., Gaudet, B. J., Miles, N., Richardson, S. J., Wu, K., Sarmiento, D. P., Hardesty, R. M., and Bonin, T. A.: Toward reduced transport errors in a high resolution urban CO_2 inversion system, Elem. Sci. Anth., 5, 2017.

Efron, B., and Tibshirani, R.: Bootstrap methods for standard errors, confidence intervals, and other measures of statistical accuracy, Statist. Sci., 1, 54-75, 10.1214/ss/1177013815, 1986.

Gurney, K. R., Razlivanov, I., Song, Y., Zhou, Y., Benes, B., and Abdul-Massih, M.: Quantification of fossil fuel CO_2 emissions on the building/street scale for a large U.S. city, Environmental Science & Technology, 46, 12194-12202, 10.1021/es3011282, 2012.

Hanna, S. R., Briggs, G. A., and Hosker Jr, R. P.: Handbook on atmospheric diffusion, National Oceanic and Atmospheric Administration, Oak Ridge, TN (USA). Atmospheric Turbulence and Diffusion Lab., 1982.

Heimburger, A. M., Harvey, R. M., Shepson, P. B., Stirm, B. H., Gore, C., Turnbull, J., Cambaliza, M. O., Salmon, O. E., Kerlo, A.-E. M., and Lavoie, T. N.: Assessing the optimized precision of the aircraft mass balance method for measurement of urban greenhouse gas emission rates through averaging, Elem. Sci. Anth., 5, 2017.

Helfter, C., Tremper, A. H., Halios, C. H., Kotthaus, S., Bjorkegren, A., Grimmond, C. S. B., Barlow, J. F., and Nemitz, E.: Spatial and temporal variability of urban fluxes of methane, carbon monoxide and carbon dioxide above London, UK, Atmos. Chem. Phys., 16, 10543-10557, 10.5194/acp-16-10543-2016, 2016.

Hendrick, M. F., Ackley, R., Sanaie-Movahed, B., Tang, X., and Phillips, N. G.: Fugitive methane emissions from leak-prone natural gas distribution infrastructure in urban environments, Environmental Pollution, 213, 710-716, https://doi.org/10.1016/j.envpol.2016.01.094, 2016.

687 Hiller, R. V., Neininger, B., Brunner, D., Gerbig, C., Bretscher, D., Künzle, T., Buchmann, N.,
688 and Eugster, W.: Aircraft-based CH_4 flux estimates for validation of emissions from an
689 agriculturally dominated area in Switzerland, Journal of Geophysical Research:
690 Atmospheres, 119, 4874-4887, doi:10.1002/2013JD020918, 2014.
691 Jackson, R. B., Down, A., Phillips, N. G., Ackley, R. C., Cook, C.W., Plata, D. L., and Zhao, K.
692 G.: Natural gas pipeline leaks across Washington, DC, Environ. Sci. Technol., 48, 2051–
693 2058, doi:10.1021/es404474x, 2014.
694 Jeong, S., Millstein, D., and Fischer, M. L.: Spatially explicit methane emissions from petroleum
695 production and the natural gas system in California, Environmental Science &
696 Technology, 48, 5982-5990, 10.1021/es4046692, 2014.
697 Jeong, S., Newman, S., Zhang, J., Andrews, A. E., Bianco, L., Bagley, J., Cui, X., Graven, H.,
698 Kim, J., Salameh, P., LaFranchi, B. W., Priest, C., Campos-Pineda, M., Novakovskaia,
699 E., Sloop, C. D., Michelsen, H. A., Bambha, R. P., Weiss, R. F., Keeling, R., and Fischer,
700 M. L.: Estimating methane emissions in California's urban and rural regions using
701 multitower observations, Journal of Geophysical Research: Atmospheres, 121, 13,031-
702 013,049, doi:10.1002/2016JD025404, 2016.
703 Jeong, S., Cui, X., Blake, D. R., Miller, B., Montzka, S. A., Andrews, A., Guha, A., Martien, P.,
704 Bambha, R. P., LaFranchi, B., Michelsen, H. A., Clements, C. B., Glaize, P., and Fischer,
705 M. L.: Estimating methane emissions from biological and fossil-fuel sources in the San
706 Francisco Bay Area, Geophysical Research Letters, 44, 486-495,
707 doi:10.1002/2016GL071794, 2017.
708 Karion, A., Sweeney, C., Kort, E. A., Shepson, P. B., Brewer, A., Cambaliza, M., Conley, S. A.,
709 Davis, K., Deng, A., Hardesty, M., Herndon, S. C., Lauvaux, T., Lavoie, T., Lyon, D.,
710 Newberger, T., Pétron, G., Rella, C., Smith, M., Wolter, S., Yacovitch, T. I., and Tans,
711 P.: Aircraft-based estimate of total methane emissions from the Barnett Shale region,
712 Environ. Sci. Technol., 49, 8124–8131, doi:10.1021/acs.est.5b00217, 2015
713 Kort, E. A., Eluszkiewicz, J., Stephens, B. B., Miller, J. B., Gerbig, C., Nehrkorn, T., Daube, B.
714 C., Kaplan, J. O., Houweling, S., and Wofsy, S. C.: Emissions of CH_4 and N_2O over the
715 United States and Canada based on a receptor-oriented modeling framework and
716 COBRA-NA atmospheric observations, Geophys. Res. Lett., 35, L18808,
717 doi:10.1029/2008GL034031, 2008.

718 Lamb, B. K., Cambaliza, M. O. L., Davis, K. J., Edburg, S. L., Ferrara, T. W., Floerchinger, C.,
719 Heimburger, A. M. F., Herndon, S., Lauvaux, T., Lavoie, T., Lyon, D. R., Miles, N.,
720 Prasad, K. R., Richardson, S., Roscioli, J. R., Salmon, O. E., Shepson, P. B., Stirm, B. H.,
721 and Whetstone, J.: Direct and indirect measurements and modeling of methane emissions
722 in Indianapolis, Indiana, Environmental Science & Technology, 50, 8910-8917,
723 10.1021/acs.est.6b01198, 2016.
724 Lauvaux, T., Miles, N. L., Deng, A., Richardson, S. J., Cambaliza, M. O., Davis, K. J., Gaudet,
725 B., Gurney, K. R., Huang, J., O'Keefe, D., Song, Y., Karion, A., Oda, T., Patarasuk, R.,
726 Razlivanov, I., Sarmiento, D., Shepson, P., Sweeney, C., Turnbull, J., and Wu, K.: High-
727 resolution atmospheric inversion of urban CO_2 emissions during the dormant season of
728 the Indianapolis Flux Experiment (INFLUX), Journal of Geophysical Research:
729 Atmospheres, 121, 5213-5236, doi:10.1002/2015JD024473, 2016.
730 Maasakkers, J. D., Jacob, D. J., Sulprizio, M. P., Turner, A. J., Weitz, M., Wirth, T., Hight, C.,
731 DeFigueiredo, M., Desai, M., Schmeltz, R., Hockstad, L., Bloom, A. A., Bowman, K.
732 W., Jeong, S., and Fischer, M. L.: Gridded national inventory of U.S. methane emissions,
733 Environmental Science & Technology, 50, 13123-13133, 10.1021/acs.est.6b02878, 2016.
734 Mays, K. L., Shepson, P. B., Stirm, B. H., Karion, A., Sweeney, C., and Gurney, K. R.: Aircraft-
735 based measurements of the carbon footprint of Indianapolis, Environmental Science &
736 Technology, 43, 7816-7823, 10.1021/es901326b, 2009.
737 McKain, K., Down, A., Raciti, S. M., Budney, J., Hutyra, L. R., Floerchinger, C., Herndon, S.
738 C., Nehrkorn, T., Zahniser, M. S., Jackson, R. B., Phillips, N., and Wofsy, S. C.: Methane
739 emissions from natural gas infrastructure and use in the urban region of Boston,
740 Massachusetts, Proceedings of the National Academy of Sciences, 112, 1941-1946,
741 10.1073/pnas.1416261112, 2015.
742 Miles, N. L., Richardson, S. J., Lauvaux, T., Davis, K. J., Balashov, N. V., Deng, A., Turnbull, J.
743 C., Sweeney, C., Gurney, K. R., and Patarasuk, R.: Quantification of urban atmospheric
744 boundary layer greenhouse gas dry mole fraction enhancements in the dormant season:
745 Results from the Indianapolis Flux Experiment (INFLUX), Elem. Sci. Anth., 5, 2017.
746 Miller, S. M., Wofsy, S. C., Michalak, A. M., Kort, E. A., Andrews, A. E., Biraud, S. C.,
747 Dlugokencky, E. J., Eluszkiewicz, J., Fischer, M. L., Janssens-Maenhout, G., Miller, B.
748 R., Miller, J. B., Montzka, S. A., Nehrkorn, T., and Sweeney, C.: Anthropogenic

749 emissions of methane in the United States, Proceedings of the National Academy of
750 Sciences, 110, 20018-20022, 10.1073/pnas.1314392110, 2013.
751 Myhre, G., Shindell, D., Bréon, F. M., Collins, W., Fuglestvedt, J., Huang, J., Koch, D.,
752 Lamarque, J. F., Lee, D., Mendoza, B., Nakajima, T., Robock, A., Stephens, G.,
753 Takemura, T., and Zhang, H.: Anthropogenic and natural radiative forcing, in: Climate
754 Change 2013: The Physical Science Basis. Contribution of Working Group I to the Fifth
755 Assessment Report of the Intergovernmental Panel on Climate Change, edited by:
756 Stocker, T. F., Qin, D., Plattner, G. K., Tignor, M., Allen, S. K., Doschung, J., Nauels,
757 A., Xia, Y., Bex, V., and Midgley, P. M., Cambridge University Press, Cambridge, UK,
758 659-740, 2013.
759 National Academies of Sciences and Medicine: Improving characterization of anthropogenic
760 methane emissions in the United States, The National Academies Press, Washington, DC,
761 250 pp., 2018.
762 Nisbet, E. G., Dlugokencky, E. J., Manning, M. R., Lowry, D., Fisher, R. E., France, J. L.,
763 Michel, S. E., Miller, J. B., White, J. W. C., Vaughn, B., Bousquet, P., Pyle, J. A.,
764 Warwick, N. J., Cain, M., Brownlow, R., Zazzeri, G., Lanoisellé, M., Manning, A. C.,
765 Gloor, E., Worthy, D. E. J., Brunke, E.-G., Labuschagne, C., Wolff, E. W., and Ganesan,
766 A. L.: Rising atmospheric methane: 2007–2014 growth and isotopic shift, Global
767 Biogeochemical Cycles, 30, 1356-1370, doi:10.1002/2016GB005406, 2016.
768 Richardson, S. J., Miles, N. L., Davis, K. J., Lauvaux, T., Martins, D. K., Turnbull, J. C.,
769 McKain, K., Sweeney, C., and Cambaliza, M. O. L.: Tower measurement network of in-
770 situ CO_2, CH_4, and CO in support of the Indianapolis FLUX (INFLUX) Experiment,
771 Elem Sci Anth, 5, 2017.
772 Sarmiento, D. P., Davis, K. J., Deng, A., Lauvaux, T., Brewer, A., and Hardesty, M.: A
773 comprehensive assessment of land surface-atmosphere interactions in a WRF/Urban
774 modeling system for Indianapolis, IN, Elem. Sci. Anth., 5, 2017.
775 Saunois, M., Jackson, R. B., Bousquet, P., Poulter, B., and Canadell, J. G.: The growing role of
776 methane in anthropogenic climate change, Environmental Research Letters, 11, 120207,
777 2016.
778 Schuh, A. E., Lauvaux, T., West, T. O., Denning, A. S., Davis, K. J., Miles, N., Richardson, S.,
779 Uliasz, M., Lokupitiya, E., Cooley, D., Andrews, A., and Ogle, S.: Evaluating

780 atmospheric CO_2 inversions at multiple scales over a highly inventoried agricultural
781 landscape, Global change biology, 19, 1424-1439, doi:10.1111/gcb.12141, 2013.
782 Taylor, D. M., Chow, F. K., Delkash, M., and Imhoff, P. T.: Atmospheric modeling to assess
783 wind dependence in tracer dilution method measurements of landfill methane emissions,
784 Waste Management, 73, 197-209, https://doi.org/10.1016/j.wasman.2017.10.036, 2018.
785 Townsend-Small, A., Tyler, S. C., Pataki, D. E., Xu, X., and Christensen, L. E.: Isotopic
786 measurements of atmospheric methane in Los Angeles, California, USA: Influence of
787 "fugitive" fossil fuel emissions, J. Geophys. Res.-Atmos., 117, 1–11,
788 https://doi.org/10.1029/2011JD016826, 2012.
789 Turnbull, J. C., Sweeney, C., Karion, A., Newberger, T., Lehman, S. J., Tans, P. P., Davis, K. J.,
790 Lauvaux, T., Miles, N. L., Richardson, S. J., Cambaliza, M. O., Shepson, P. B., Gurney,
791 K., Patarasuk, R., and Razlivanov, I.: Toward quantification and source sector
792 identification of fossil fuel CO_2 emissions from an urban area: Results from the INFLUX
793 experiment, Journal of Geophysical Research: Atmospheres, 120, 292-312,
794 doi:10.1002/2014JD022555, 2015.
795 Turnbull, J. C., Karion, A., Davis, K. J., Lauvaux, T., Miles, N. L., Richardson, S. J., Sweeney,
796 C., McKain K., Lehman, S. J., Gurney, K., Patarasuk, R., Jianming L., Shepson, P. B.,
797 Heimburger A., Harvey, R., and Whetstone, J.: Synthesis of urban CO_2 emission
798 estimates from multiple methods from the Indianapolis Flux Project (INFLUX),
799 Environmental Science and Technology, 53 (1), 287-295, 10.1021/acs.est.8b05552, 2019.
800 Van De Wiel, B. J. H. V. d., Moene, A. F., Jonker, H. J. J., Baas, P., Basu, S., Donda, J. M. M.,
801 Sun, J., and Holtslag, A. A. M.: The minimum wind speed for sustainable turbulence in
802 the nocturnal boundary layer, Journal of the Atmospheric Sciences, 69, 3116-3127,
803 10.1175/jas-d-12-0107.1, 2012.
804 Wunch, D., Wennberg, P. O., Toon, G. C., Keppel-Aleks, G., and Yavin, Y. G.: Emissions of
805 greenhouse gases from a North American megacity, Geophysical Research Letters, 36,
806 doi:10.1029/2009GL039825, 2009.
807 Zavala-Araiza, D., Lyon, D. R., Alvarez, R. A., Davis, K. J., Harriss, R., Herndon, S. C., Karion,
808 A., Kort, E. A., Lamb, B. K., Lan, X., Marchese, A. J., Pacala, S. W., Robinson, A. L.,
809 Shepson, P. B., Sweeney, C., Talbot, R., Townsend-Small, A., Yacovitch, T. I.,
810 Zimmerle, D. J., and Hamburg, S. P.: Reconciling divergent estimates of oil and gas

methane emissions, Proceedings of the National Academy of Sciences, 112, 15597-15602, 10.1073/pnas.1522126112, 2015.

Tables

Table 1. INFLUX towers used to estimate CH_4 background based on two different criteria. Numbers in bold indicate towers chosen to generate a background field when multiple options are possible (for more details see discussion). In short, criterion 1 uses towers with the lowest mean CH_4 for a specific wind direction, and criterion 2 uses towers outside of Marion County and not downwind of large sources (including the city as a whole).

Wind Direction	CH_4 Background Towers	
	Criterion 1	Criterion 2
North (N)	8	**13**, 8
Northeast (NE)	8	**13**, 8, 2
East (E)	**2**, 8	**8**, 4, 1, 2
Southeast (SE)	1	**8**, 13, 4, 1
South (S)	1	**4**, 13, 1
Southwest (SW)	13	**1**, 4
West (W)	1	**4**, 1
Northwest (NW)	1	**8**, 1

Table 2. A number of independent samples needed (column 4) to satisfy combined requirement of 6 ppb background error based on the sum of bias and random error (explained in section 3.2) as a function of wind direction.

Wind Direction	Bias (ppb)	Threshold (ppb)	Samples Needed
N	1	5	74
NE	1	5	36
E	0.5	5.5	46
SE	4	2	>150
S	2	4	53
SW	4.5	1.5	>150
W	3	3	52
NW	5	1	>150

Figures

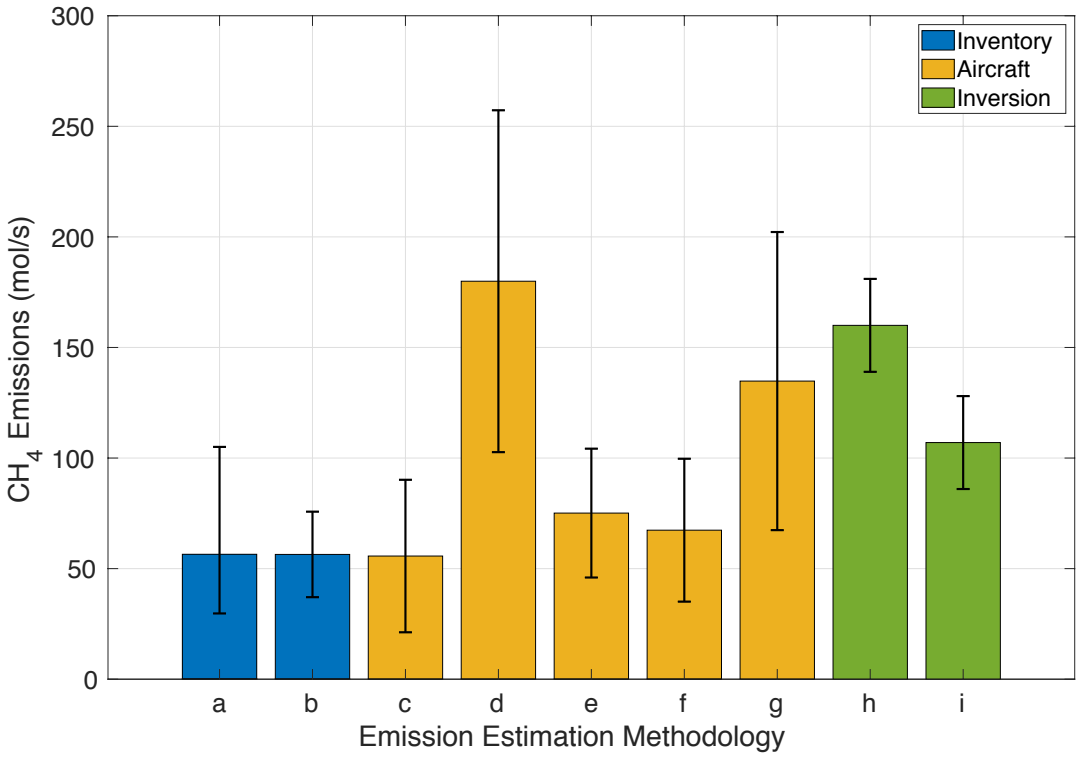

Figure 1. Various estimates of CH_4 emissions at Indianapolis. **(a, b)** Bottom-up estimates of CH_4 emissions conducted by Lamb et al. (2016) in 2013 and Maasakkers et al. (2016) based on the EPA 2012 inventory respectively. Error bars show 95% confidence intervals (for more details see above-mentioned articles). **(c-g)** Top-down evaluations of CH_4 emissions with aircraft from various flight campaigns where **(c)** contains 5 flights over March-April of 2008, **(d)** contains 3 flights over November-January of 2008-09, **(e)** contains 5 flights over April-July of 2011, **(f)** contains 9 flights from November-December, 2014, and **(g)** contains the same 5 flights over April-July of 2011 as in (e) but uses different methodology. Methodologies for **(c-f)** are described in Lamb et al. (2016) and methodology for **(g)** is described in Cambaliza et al. (2015). Error bars show 95% confidence intervals (for more details see above-mentioned articles). **(h, i)** Top-down evaluations of CH_4 emissions for 2012-2013 using tower inversion modeling methodology with two different domains, where **(h)** uses the full domain of Figure 2 and **(i)** uses only the Marion County domain of Figure 2. The inversion methodology and 95% confidence intervals are described in detail in Lamb et al. (2016).

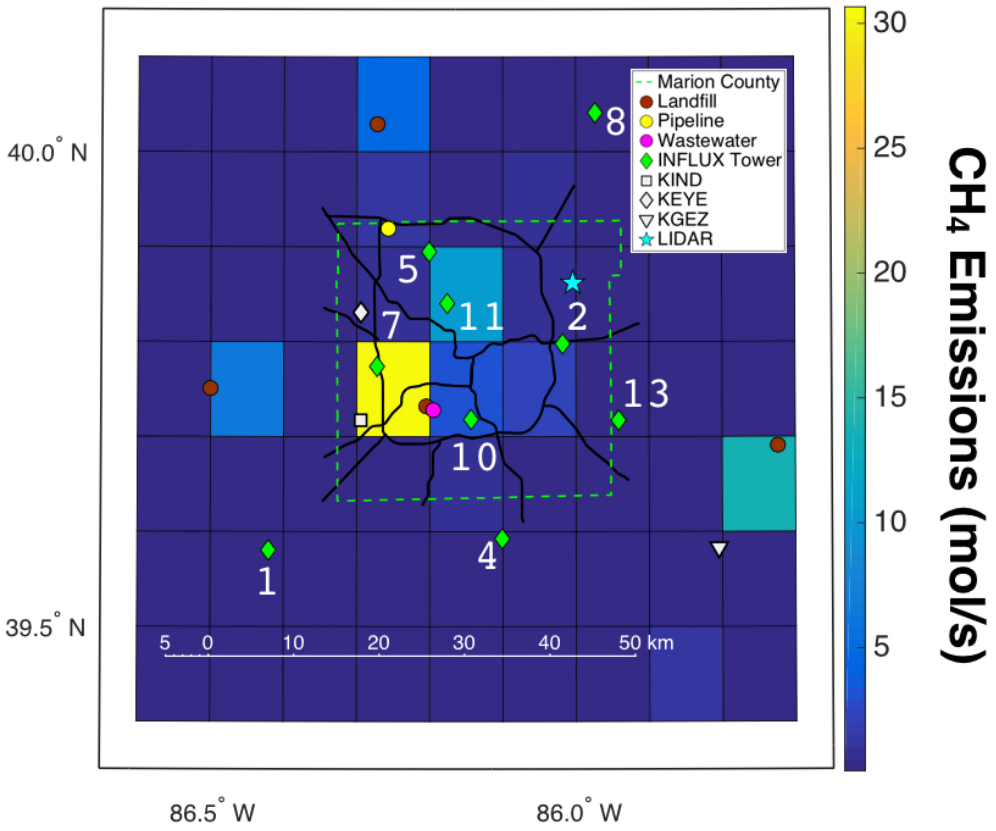

935

936 **Figure 2.** Map of the primary roads in Indianapolis, INFLUX towers, lidar system, weather stations, and
937 a few CH_4 point sources plotted over the gridded CH_4 emissions (mol/s) from the EPA 2012 Inventory
938 (Maasakkers et al., 2016). The gridded map of emissions includes emissions from the mentioned point
939 sources; their position is provided to aid in interpretation of the observations. The dashed bright green
940 line denotes Marion County borders.

941

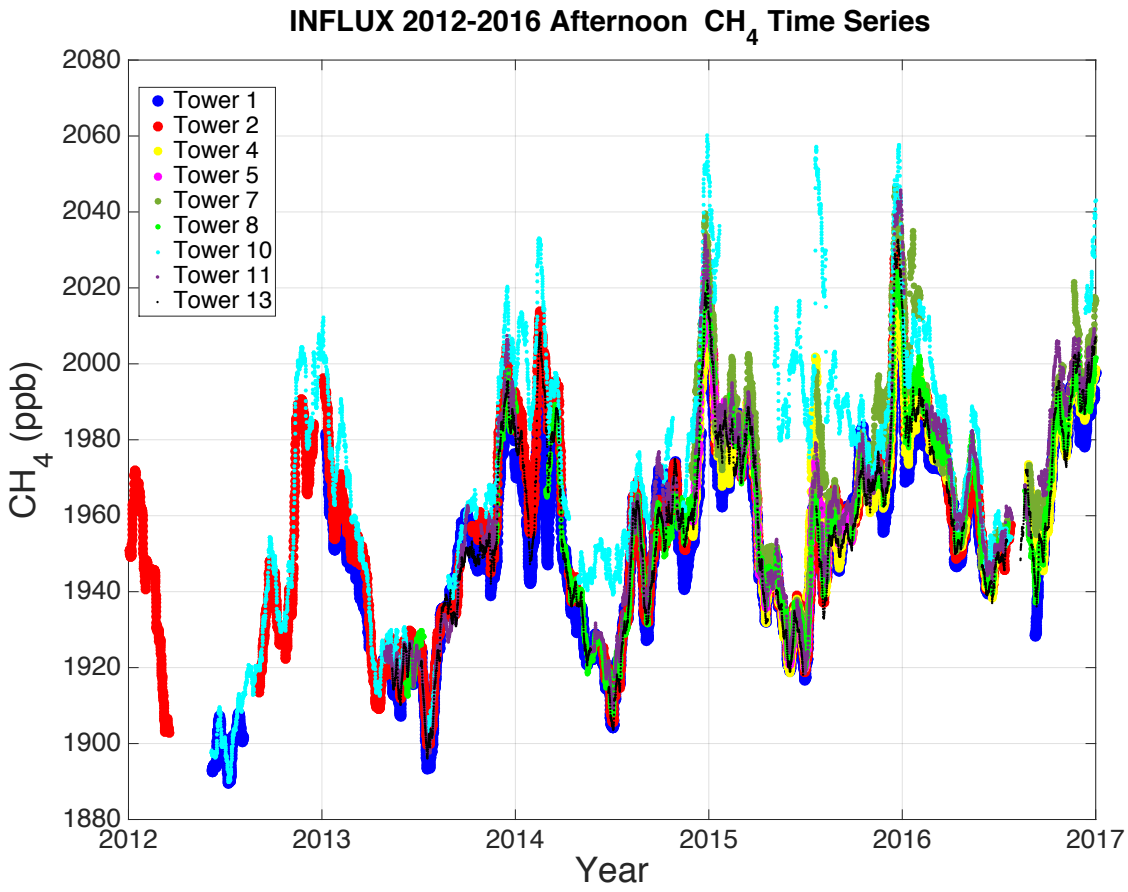

942

943 **Figure 3.** 20-day running average of afternoon (12-16 LST; the hours are inclusive) CH_4 mole fractions
944 as measured by the INFLUX tower network (highest available height is used) from 2012 through 2016.

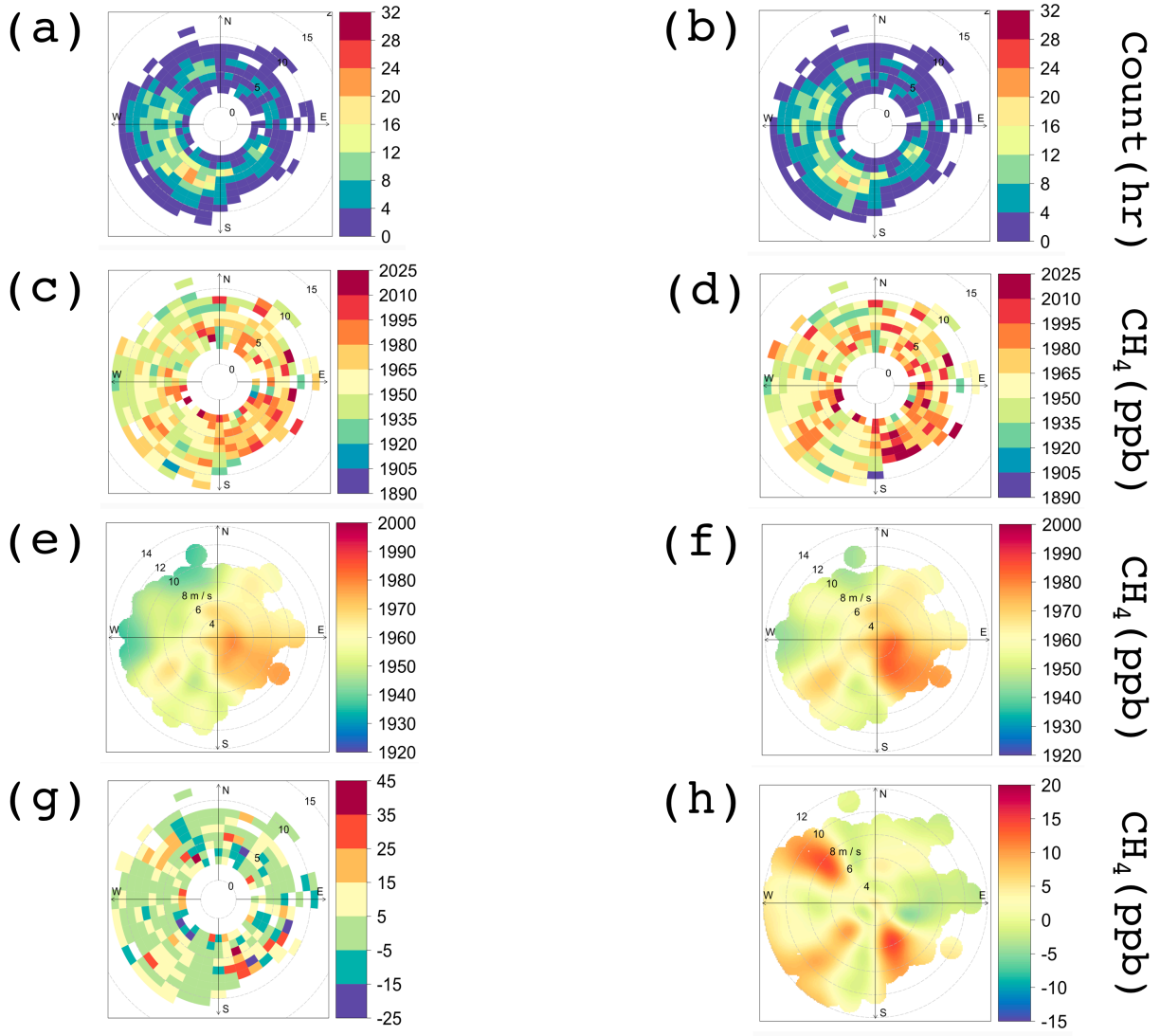

945

946 **Figure 4.** Frequency and bivariate polar plots of CH_4 background for Indianapolis using data from 12-16
947 LST, November 2014 through December 2016 given 2 different criteria (Table 1). **(a)** Polar histogram
948 indicating a number of hourly measurements available using criterion 1. **(b)** Same as (a) only for criterion
949 2. Differences between (a) and (b) are due to slight differences in data availability at the considered
950 towers. **(c)** Polar frequency plot of the CH_4 background using criterion 1. **(d)** Same as (c) only for
951 criterion 2. **(e)** Polar bivariate plot of CH_4 background using criterion 1. **(f)** Same as (e) only for criterion
952 2. **(g)** Polar frequency plot of difference between the backgrounds: $criterion\ 2 - criterion\ 1$. **(h)** Same
953 as (g) but shown with a bivariate polar plot.

954

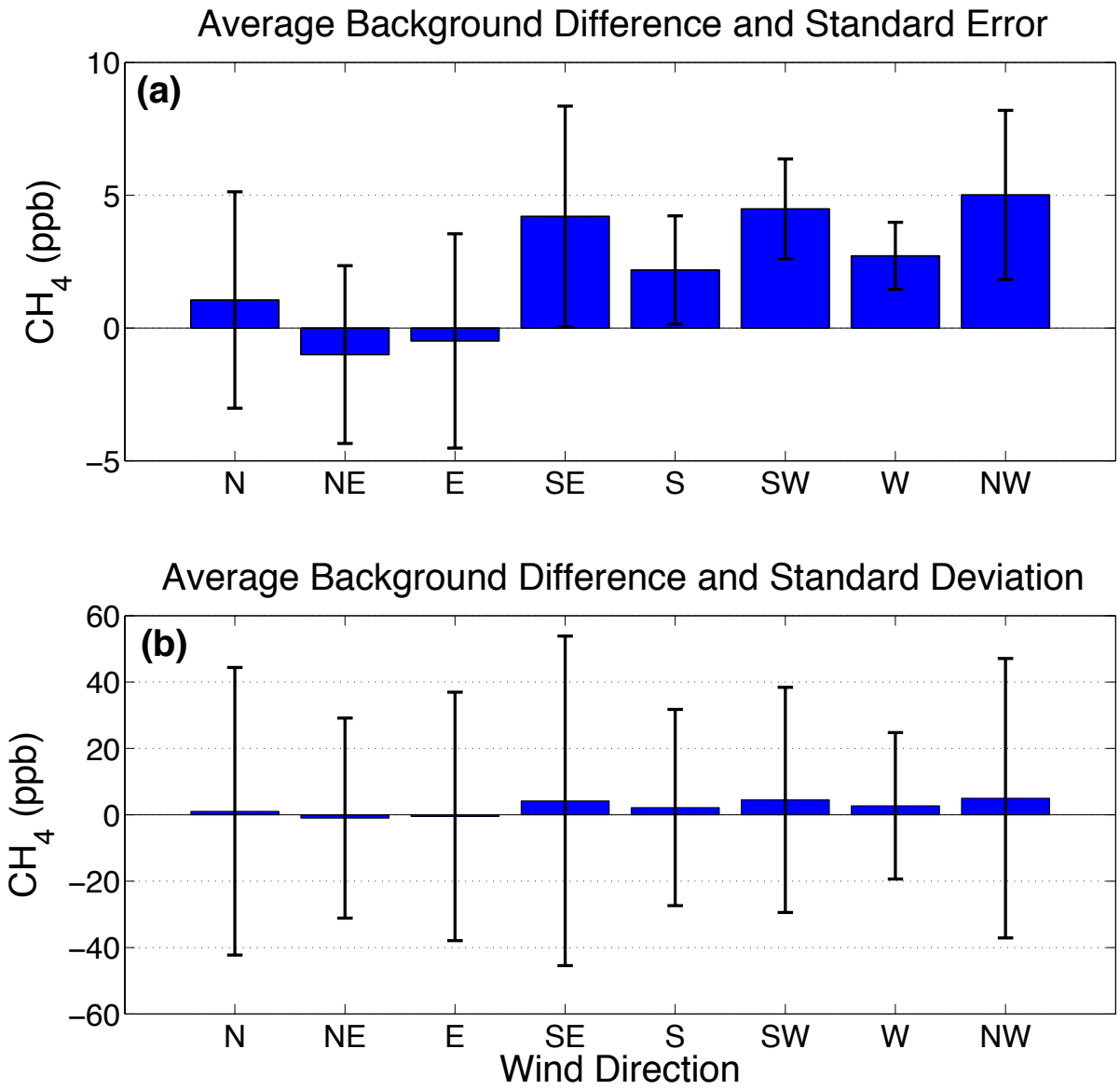

Figure 5. Average of the differences between criteria 2 and 1 CH_4 backgrounds at Indianapolis as a function of wind direction. These averages are generated from the same data that is used in Figure 4 and reflect results shown in Figure 4g. Error bars indicate in (a) 2 × standard error and in (b) 2 × standard deviation.

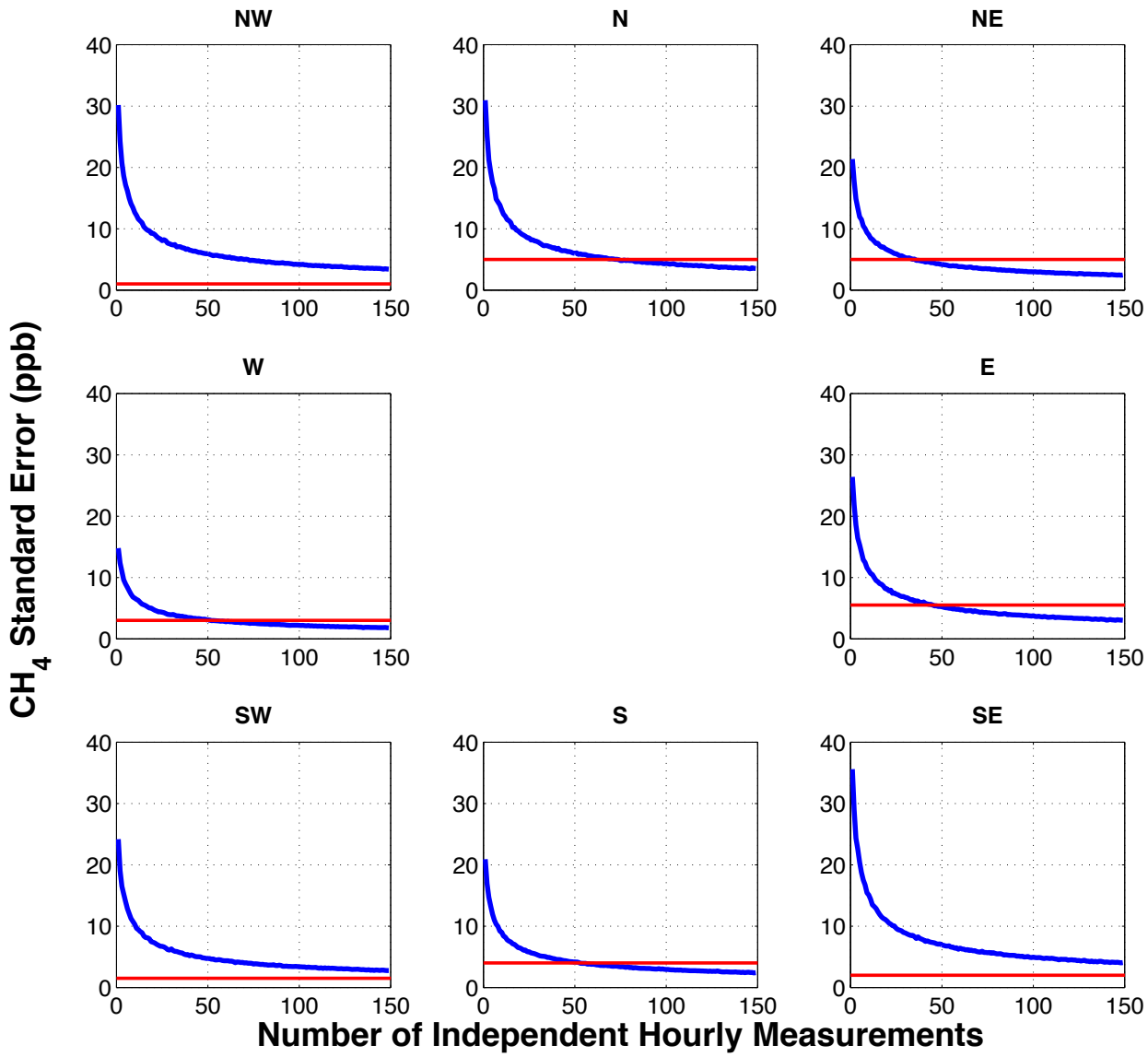

Figure 6. Bootstrap simulation of the standard errors × 2 in Indianapolis CH_4 background mole fraction differences (between criteria 2 and 1) as a function of sample size and wind direction (see text for details). Thresholds for each of the wind directions indicate a random error threshold needed for the background uncertainty to be within 50% of Indianapolis CH_4 enhancement of 12 ppb.

966

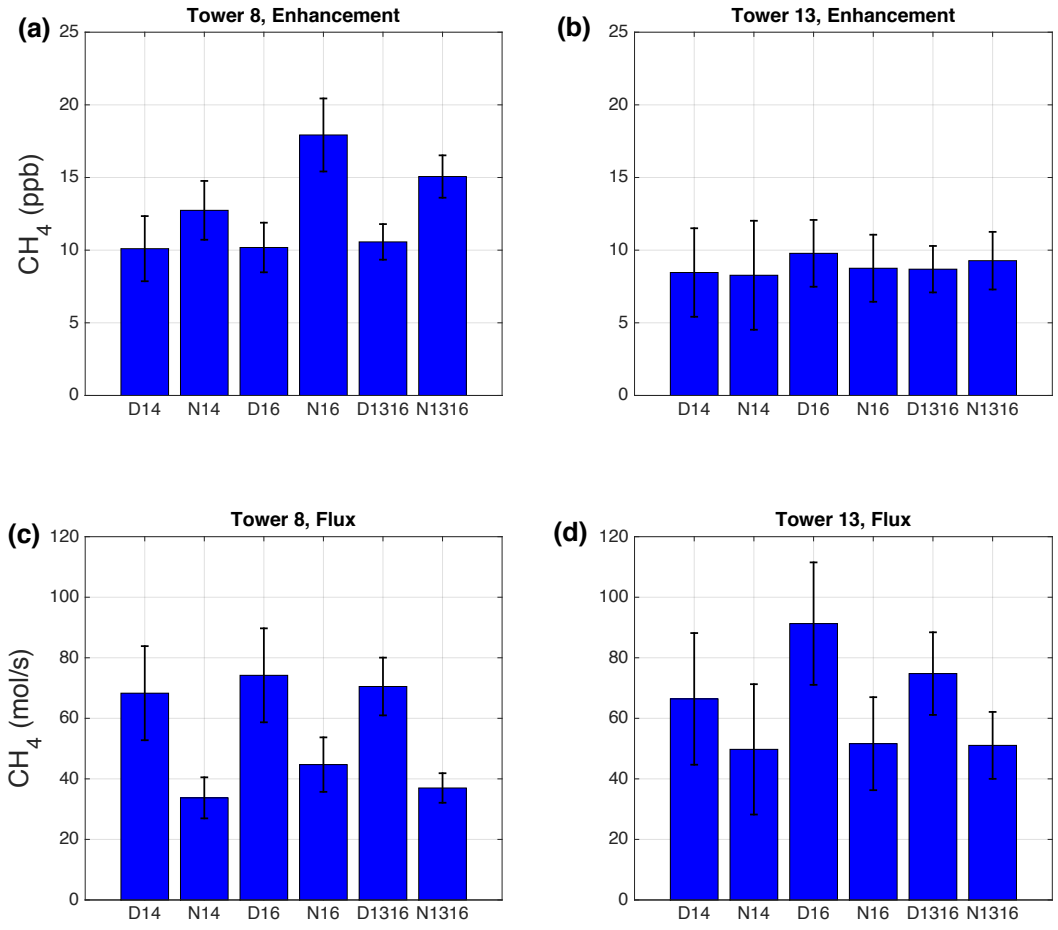

967

968 **Figure 5.** Averages of the daytime (D) and nighttime (N) CH_4 enhancements and fluxes at INFLUX
969 towers 8 and 13 for years 2014 (14), 2016 (16), and 2013-2016 (1316). The error bars represent 95%
970 confidence interval of each mean value. **(a)** Estimates of CH_4 enhancements from tower 8. **(b)** Estimates
971 of CH_4 enhancements from tower 13. **(c)** Estimates of CH_4 flux from tower 8. **(d)** Estimates of CH_4 flux
972 from tower 13.

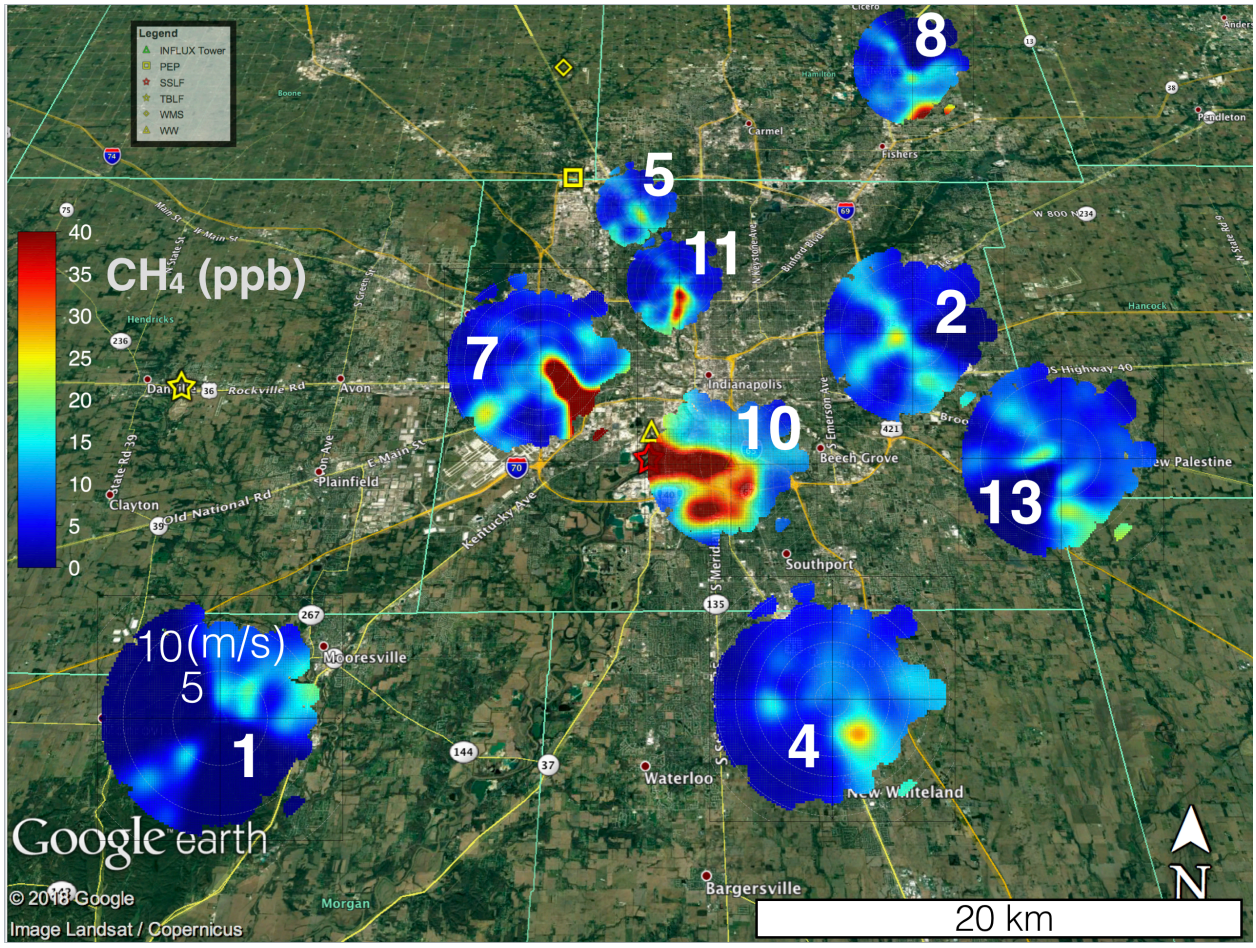

Figure 6. Google Earth image overlaid with bivariate polar plots (section 2.5) of the CH_4 enhancements at 9 INFLUX towers in Indianapolis using the criterion 1 background (Table 1) for full years of 2014 and 2015 over the afternoon (12-16 LST). The wind speed scale is only labeled at site 1; other sites follow the same convention. Legend indicates known sources of CH_4: Panhandle Eastern Pipeline (PEP), Southern Side Landfill (SSLF), Twin Bridges Landfill (TBLF), Waste Management Solutions (WMS), and Waste Water treatment facility (WW). The known magnitudes of sources that are in Marion County (PEP, SSLF, and WW) are reported in section 2.7. Magnitudes of TBLF and WMS according to EPA are approximately 5 mol/s. The largest known source on the map is SSLF.

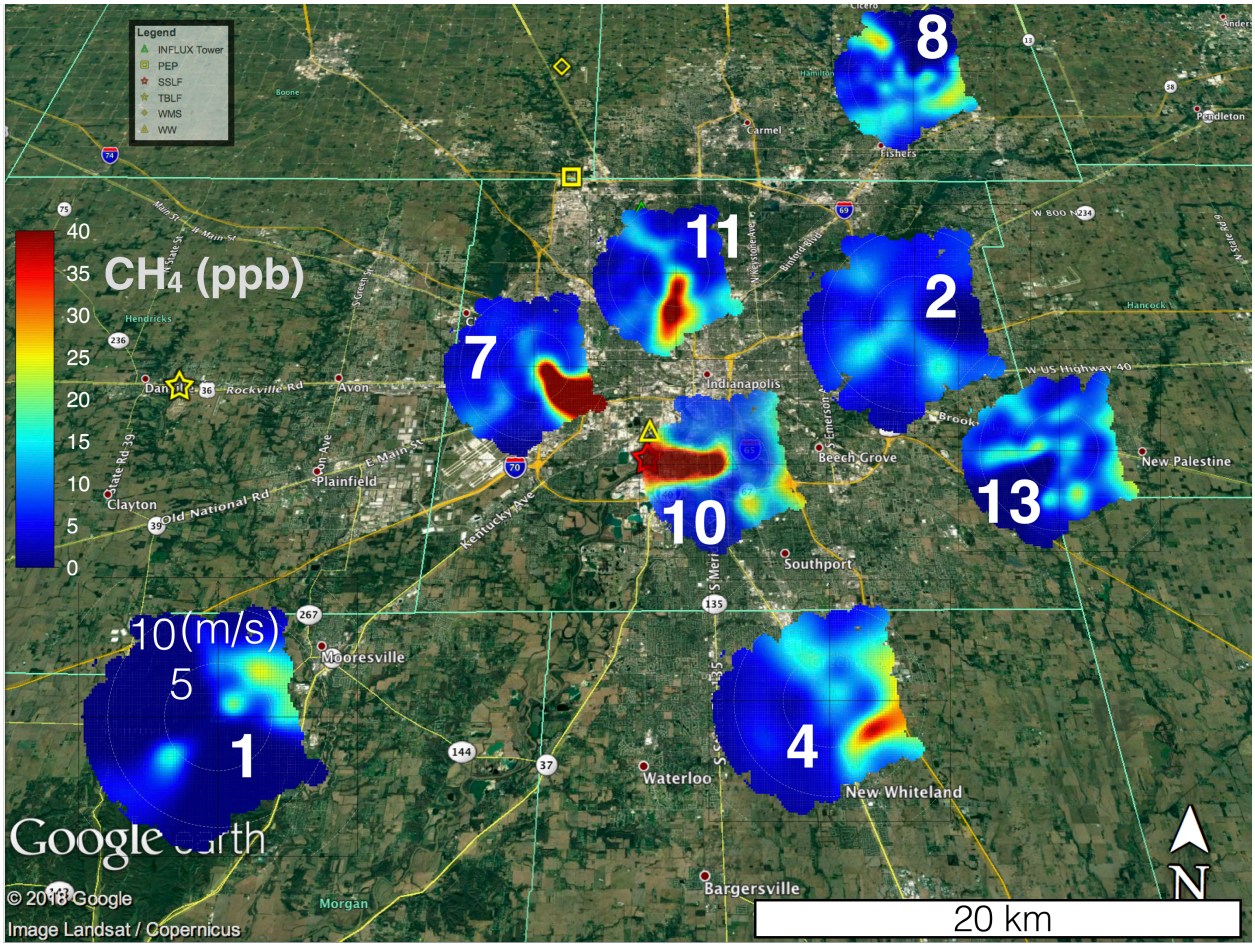

Figure 7. Google Earth image overlaid with bivariate polar plots (section 2.5) of the CH_4 enhancements at 9 INFLUX towers in Indianapolis using the criterion 1 background (Table 1) for year 2016 over the afternoon (12-16 LST). The wind speed scale is only labeled at site 1; other sites follow the same convention. Legend indicates known sources of CH_4: Panhandle Eastern Pipeline (PEP), Southern Side Landfill (SSLF), Twin Bridges Landfill (TBLF), Waste Management Solutions (WMS), and Waste Water treatment facility (WW). The known magnitudes of sources that are in Marion County (PEP, SSLF, and WW) are reported in section 2.7. Magnitudes of TBLF and WMS according to EPA are approximately 5 mol/s. The largest known source on the map is SSLF.